First-principles stability study of olivine $NaMPO_4$ (M: Mn, Fe, Co)

NL Lethole, HR Chauke and PE Ngoepe
Materials Modelling Centre, University of Limpopo, Private Bag X1106, Sovenga, 0727, South Africa
E-mail: Lesley.lethole@ul.ac.za

Abstract. First-principles calculations were carried out to investigate the structural, thermodynamic, electronic and mechanical properties of olivine $NaMPO_4$. All calculations were performed using plane-wave pseudopotential method within the generalised gradient approximation (GGA) functional with Hubbard *U* correction. We note that the calculated lattice parameters are in good agreement to within 6 % with the experimental data. The predicted heats of formation suggest that $NaMnPO_4$ is the most thermodynamic stable structure, with the lowest formation energy (-1292 kJ/mol). The calculated density of states showed that Fe 3*d* states for the $NaFePO_4$ system overlap the Fermi level E_F, suggesting a semi-metallic behaviour leading to good electronic conductivity. On the other hand, $NaCoPO_4$ and $NaMnPO_4$ show insulator behaviour due to the existence of energy band gap around the Fermi Level. Lastly, all the independent elastic constants for all structures satisfy the necessary stability criterion, indicating that all $NaMPO_4$ structures are mechanically stable.

1. Introduction

Sodium transition metal phosphates ($NaMPO_4$), with olivine structure, have recently attracted a lot of interest in battery applications as potential candidates for future cathode battery material. However, very little work has been done on the sodium-based material as many studies have primarily focused on well-developed counterpart, olivine lithium metal phosphates ($LiMPO_4$), due to the significant discoveries and investigations on lithium ion batteries [1, 2, 3, 4, 5]. Concerns regarding the abundance and possibilities of drastically increase in lithium ion batteries prices when demand intensifies may arise. Unlike the olivine $LiMPO_4$, the sodium-based olivine transition metal phosphates are more abundant and inexhaustible in the world [6].

Figure 1 shows the simulation models for olivine $NaMPO_4$ with space group *Pnma*. The M atoms are located in the octahedral sites, while P atoms occupy tetrahedral sites with a distorted hexagonal close-packed framework. The framework is coordinated by oxygen atoms forming layers of edge-sharing MO_6 octahedra, separated by PO_4 tetrahedra. Na ions move within the one-dimensional tunnel formed by the edge sharing LiO_6 octahedrons.

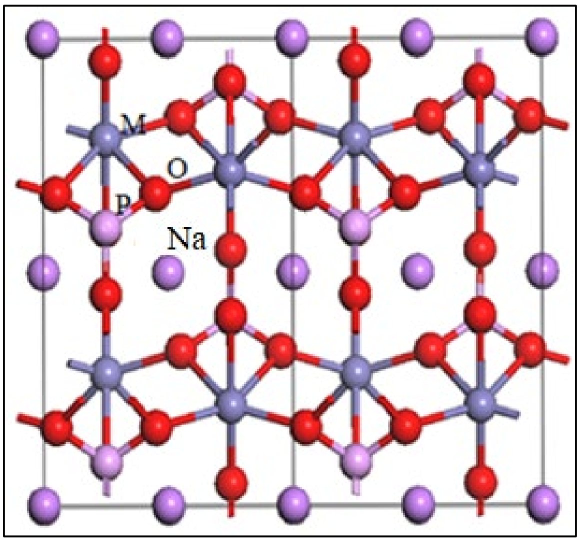

Figure 1 Atomic arrangement of $NaMPO_4$ olivines structures.

The major drawback for the sodium metal phosphates has been their low charge/discharge capacities. Previous studies by Shakoor *et al.* [7] reported that $NaFePO_4$ and $NaCoPO_4$ offer charge/discharge capacities of 12 mAh/g and 2.0 mAh/g, respectively, which is very less compared to the olivine $LiFePO_4$ (170 mAh/g) [8, 9], $LiMnPO_4$ (165 mAh/g) [10] and $LiCoPO_4$ (70 - 86 mAh/g) [9] and other sodium based cathode materials such as $Na_{1.5}VOPO_4F_{0.5}$ (80 mAh/g) and $Na_3V_2(PO_4)F_3$ (90 mAh/g) [11]. Several studies have suggested that the low capacities may be attributed to slow diffusion kinetics of sodium into the structure and the closed packed crystal structure which causes the sodium ion immobility [7, 12]. On the other hand, a study by Sun and Manivannan have shown that the $NaFePO_4$ electrode is capable of maintaining capacity for a large number of cycles, despite low capacity. It was reported that the charge/discharge densities continued to increase for more than 300 cycles [13], making this material a good candidate for large scale energy storage systems for smart grid applications. In addition, studies are required to enhance the $NaMPO_4$ electrochemical activity at room temperature, an important attribute for producing better sodium ion batteries.

Previous studies have reported the maricite $NaFePO_4$ to be seemingly the most thermodynamically stable phase as compared to olivine. It is reported that the maricite phase is 0.016 eV/formula unit more stable than the olivine [6, 14]. However, the edge-sharing FeO_6 octahedrons and lack of cationic channels for Na diffusion make this material an unlikely candidate for sodium ion battery development. In this study, we investigate the structural, thermodynamic, electronic and mechanical properties for the olivine $NaMPO_4$ (M=Fe, Co, Mn) structures to determine their stability and competences as future cathode materials. The heats of formation, electronic densities of states (DOS) and elastic constants will be calculated to mimic the stability trend at 0 K.

2. Methodology

First-principles DFT+U calculations were performed using the Vienna *Ab Initio S*imulation Package, VASP [15] to determine stability of olivine $NaMPO_4$. We used the spin-polarised generalised gradient approximation (GGA). A plane-wave cut-off of 500 eV and suitable k-mesh point of 4x6x6 was chosen for geometric optimisation. The Hubbard parameter of U=5.5 eV and $J=1$ eV were found to correctly predict the lattice constants of transition metal phosphates [16]. Phonon dispersion curves were calculated with an interaction range of 7.0 Å. The DOS were calculated with the spin taken into account with a smearing width 0.05 eV using a Methfessel–Paxton smearing approach [17].

3. Results and discussion

3.1 Structural and thermodynamic properties

In table 1, we present the calculated lattice constants, heats of formation, elastic constants, moduli and Pugh ratio of $NaMPO_4$ systems. The experimental data are given in parenthesis where available. The structural lattice parameters are obtained by performing full geometry optimisation. The calculated lattice constants have been found to be in good agreement with the experimental to within 6 %, which is expected for a DFT transition metal calculation [18]. Moreover, we note that $NaMnPO_4$ (326.4 Å^3) has a larger volume over $NaFePO_4$ (318.2 Å^3) and $NaCoPO_4$ (311.7 Å^3): this may be due to the large ionic radii of Mn (81 pm) over Fe (75 pm) and Co (71 pm), respectively. The heats of formation of the $NaMPO_4$ olivines have been evaluated to mimic the thermodynamic stability using equation 1:

$$\Delta H_f\left(NaMPO_4\right)= \frac{1}{N}\left[E_{Total}-\left(E_{Na}+E_M+E_P+4E_O\right)\right], \tag{1}$$

where E_{Total} is the total energy of $NaMPO_4$, while E_{Na}, E_M, E_P and E_O are the total elemental energies of Na, Fe, P and O in their respective ground-states. We note that $NaMPO_4$ structures show relatively low heats formation, with $NaMnPO_4$ structure showing the lowest value (-1292.6 kJ/mol), suggesting stability over $NaFePO_4$ (-1143.6 kJ/mol) and $NaCoPO_4$ (-1085.5 kJ/mol), respectively. Moreover, we note that our calculated heat formation value for $NaCoPO_4$ (-1086 kJ/mol) overestimates the experimental value (-1547.5 kJ/mol) [19].

Table 1 Calculated lattice constants, heats of formation and elastic properties of olivine $NaMPO_4$ systems. Experimental data is given in parenthesis.

Structure	**a (Å)**	**b (Å)**	**c (Å)**	**V (Å^3)**	**ΔH_f (kJ/mol)**
$NaFePO_4$	9.07 (8.99)	6.90 (6.86)	5.08 (5.05)	318.26 (311.35)[a]	-1143.6
$NaCoPO_4$	8.95 (8.88)	6.86 (6.80)	5.07 (5.03)	311.68 (303.28)[b]	-1085.5 (-1547.5)
$NaMnPO_4$	9.17 (9.08)	6.92 (6.90)	5.14 (5.11)	326.38 (320.84)[c]	-1292.6

Elastic Constants (GPa)

C_{ij}	**C_{11}**	**C_{12}**	**C_{13}**	**C_{22}**	**C_{23}**	**C_{33}**	**C_{44}**	**C_{55}**	**C_{66}**
$NaFePO_4$	166.83	59.67	80.58	161.17	65.83	175.17	53.00	61.67	49.33
$NaMnPO_4$	178.17	59.83	70.17	163.67	61.50	163.33	50.33	62.33	51.33
$NaCoPO_4$	184.83	50.00	75.25	178.33	55.58	168.33	47.67	65.67	41.67

Modulus (GPa) and Pugh Ratio

	B_H	**G_H**	**E_H**	**B/G**
$NaFePO_4$	101.37	52.29	133.86	1.94
$NaMnPO_4$	98.55	53.49	135.89	1.84
$NaCoPO_4$	99.10	53.43	135.87	1.86

[a] [20] [b] [19] [c] [6]

3.2 Electronic properties

In order to gain knowledge on the electronic conductivity of $NaMPO_4$ systems as cathode materials, we have calculated their densities of states (DOS). The partial and total DOS of $NaMPO_4$ structures are presented in figure 2. We note that the total and partial DOS are separated, forming a band gap near the Fermi level (E_F). The concepts of Fermi level and band gaps are necessary to understand electronic conductivity of materials. The spin polarised densities of states calculations show that the olivines $NaMnPO_4$, $NaFePO_4$ and $NaCoPO_4$ have energy band gaps of 3.51 eV, 1.17 eV and 1.87 eV, respectively. The energy band gaps for $NaMnPO_4$ and $NaCoPO_4$ are relatively wide, suggesting insulator behaviour. $NaFePO_4$ show a relatively narrow energy band gap. Moreover, the Fermi level is located on the Fe 3*d* band, suggesting that some valence band states jumps the Fermi level barrier to the conduction band. The energy band gap value and the location of the Fermi level suggest that $NaFePO_4$ is semi-metallic leading to good electric conductivity in Na-ion batteries. The partial density of states shows that the M 3*d* states contribute significantly around the Fermi level, while Na, P and O states contribute minimally. Furthermore, we observe spin-down 3*d* peaks at about 2 eV in all systems and minimum contribution from Na, P and oxidation states. The $NaMnPO_4$ show a single 3*d* peak which may correspond to the Mn^{2+} oxidation state (most stable state), while two degenerate peaks are observed for $NaFePO_4$ suggesting Fe^{2+} and Fe^{3+} oxidation states. Clearly, Na intercalation causes the coexistence of Fe^{2+} and Fe^{3+} in the FeO_6 layers, which may have effect on charge neutrality. This may solved by extracting two electrons from O^{2-} which is reduced and released in the vacuum as O_2 [21]. As a result, the Fermi energy level shifts to higher conductive band, leading to the enhancement of electronic conductivity of $NaFePO_4$ as well as reversible capacity [22], which will be favourable for Na deintercalation. On the other hand, $NaCoPO_4$ shows only Co^{2+} states, since there is no clear distinction between the Co 3*d* peaks.

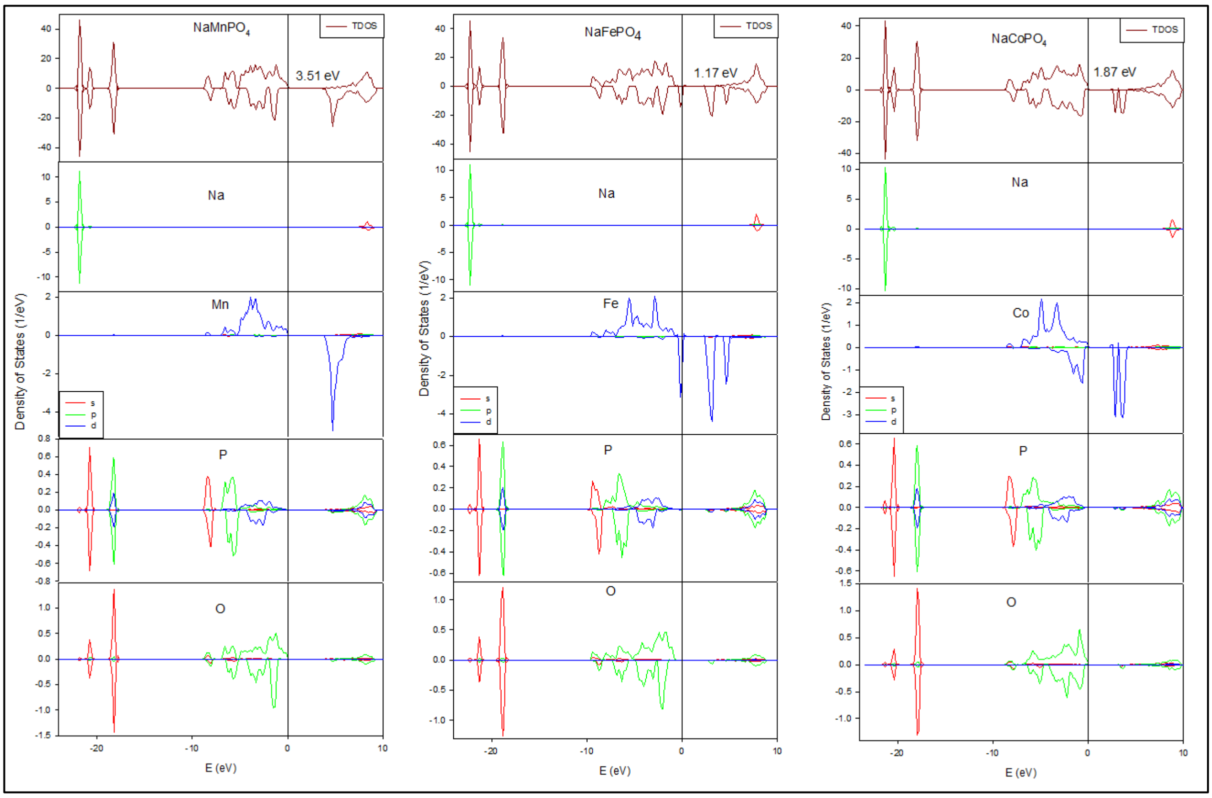

Figure 2 Partial and total density of states plots of olivine $NaMPO_4$ structures.

3.3 *Mechanical properties*

The elastic constants calculated using a Taylor expansion are presented in table 1 [23].

$$U(v,\varepsilon) = U(V_0,0) + V_0\left[\sum_i \tau_i \varepsilon_i \delta_i + \tfrac{1}{2}\sum_{ij} C_{ij}\varepsilon_i \delta_i \varepsilon_j \delta_j\right], \qquad 2$$

where $U(V_0,0)$ represents the unstrained system energy, V_0 is the equilibrium volume, τ_i is the element in the stress tensor, and δ_i is a factor of Voigt index. The orthorhombic $NaMPO_4$ structures have nine independent elastic constants (C_{ij}), which are presented in table 1. The Born mechanical stability criteria for orthorhombic systems are [24, 25]:

$$(C_{11}-C_{12})>0,\ (C_{11}+C_{33}-2C_{13})>0,\ (2C_{11}+C_{33}+2C_{12}+4C_{13})>0,$$

$$C_{11}>0,\ C_{33}>0,\ C_{44}>0,\ C_{66}>0$$

We note that all stability criteria are satisfied, indicating that $NaMPO_4$ compounds in the olivine structure are mechanically stable. To the best of our knowledge, these are the first recorded elastic constants on $NaMPO_4$ systems.

From the calculated elastic constants, the macroscopic mechanical parameters, namely, Bulk, Shear and Young's modulus are obtained using the Voigt-Reuss-Hill approach [26],

$$B_V=\frac{1}{9}(C_{11}+C_{22}+C_{33})+\frac{2}{9}(C_{12}+C_{13}+C_{23}),\ B_R=\left[(S_{11}+S_{22}+S_{33})+2(S_{12}+S_{13}+S_{23})^{-1}\right],$$

$$G_V=\frac{1}{15}(C_{11}+C_{22}+C_{33}-C_{12}-C_{13}-C_{23})+\frac{1}{5}(C_{44}+C_{55}+C_{66}),$$

$$G_R=15\left[4(S_{11}+S_{22}+S_{33})-4(S_{12}+S_{13}+S_{23})+3(S_{44}+S_{55}+S_{66})\right]^{-1},\ B_H=\frac{1}{2}(B_R+B_V),$$

$$G_{\mathrm{H}}=\frac{1}{2}(G_R+G_V),\ E_H=\frac{9B_HG_H}{G_H+3B_H},$$

where B, G and E are the bulk, shear and Young's modulus, while V, R and H are the Voigt, Reuss and Hill bounds, respectively and S_{ij} is the inverse matrix of the elastic constants matrix C_{ij}, which is given by [27];

$$S_{11}=\frac{\left(C_{22}C_{33}-C_{23}^2\right)}{\left(C_{11}C_{22}C_{33}+2C_{12}C_{13}+C_{23}-C_{11}C_{23}^2-C_{22}C_{13}^2-C_{33}C_{12}^2\right)},$$

$$S_{12}=\frac{\left(C_{13}C_{23}-C_{12}C_{33}\right)}{\left(C_{11}C_{22}C_{33}+2C_{12}C_{13}C_{23}-C_{11}C_{23}^2-C_{22}C_{13}^2-C_{33}C_{12}^2\right)},$$

$$S_{13}=\frac{\left(C_{12}C_{23}-C_{22}C_{13}\right)}{C_{11}C_{22}C_{33}+2C_{12}C_{13}C_{23}-C_{11}C_{23}^2-C_{22}C_{13}^2-C_{33}C_{12}^2},$$

$$S_{22}=\frac{\left(C_{11}C_{33}-C_{13}^2\right)}{\left(C_{11}C_{22}C_{33}+2C_{12}C_{13}C_{23}-C_{11}C_{23}^2-C_{22}C_{13}^2-C_{33}C_{12}^2\right)},$$

$$S_{23}=\frac{\left(C_{12}C_{13}-C_{11}C_{23}\right)}{\left(C_{11}C_{22}C_{33}+2C_{12}C_{13}C_{23}-C_{11}C_{23}^2-C_{22}C_{13}^2-C_{33}C_{12}^2\right)},$$

$$S_{33}=\frac{\left(C_{11}C_{22}-C_{12}^2\right)}{\left(C_{11}C_{22}C_{33}+2C_{12}C\ C_{23}-C_{11}C_{23}^2-C_{22}C_{13}^2-C_{33}C_{12}^2\right)},$$

$$S_{44}=\frac{1}{C_{44}},\ S_{55}=\frac{1}{C_{55}},\ S_{66}=\frac{1}{C_{66}}.$$

The resultant bulk, shear and Young's modulus are listed in table 1. The bulk and Young's moduli determines hardness and stiffness of the material, respectively, while the shear determines the resistance to deformation under shear stress. The bulk modulus also measure resistance to volume change under pressure [28, 29]. We note that $NaMPO_4$ structures show relatively large positive bulk, shear and Young's moduli, suggesting hardness, high resistance to volume change and deformation and stiffness, respectively. Moreover, we note that $B_H>G_H$, which implies that the parameter limiting the mechanical stability of $NaMPO_4$ structures is the shear modulus (G_H) [30]. Moreover, the Pugh criterion of ductility and brittleness was calculated. Pugh proposed that if B_H/G_H is more than the critical value (1.75), the material is ductile and if less than (1.75), the material is brittle [31]. We note all $NaMPO_4$ structures are ductile, since B_H/G_H is greater than 1.75, suggest that these materials are able to band without deformation, leading to minimal cracks during battery operation [32].

4. Conclusions

First-principles calculations on $NaMPO_4$ structures have been performed, particularly, structural parameters, heats of formation electronic density of states and elastic constants. It has been shown that the structural parameters obtained by full optimisation are in good agreement with the experimental data to within 6 %, suggesting validity of the approach employed. The heats of formation suggested thermodynamic stability of $NaMnPO_4$ structure (-1292.6 kJ/mol) over $NaFePO_4$ (-1143.6 kJ/mol) and $NaCoPO_4$ (-1085.5 kJ/mol), respectively. The electronic density of states has shown that the $NaFePO_4$ structure is semi-metallic, while $NaMnPO_4$ and $NaCoPO_4$ show insulator behaviour characteristics. The semi-metallic behaviour of $NaFePO_4$ strongly suggest that this system has better electronic conductivity, hence preferred. Lastly, the elastic properties show that the olivine $NaMPO_4$ structures are all mechanically stable and behave in a ductile manner, suggesting lack of cracks during battery operation.

Acknowledgement

This work has been performed at the Materials Modelling Centre, University of Limpopo, supported by the National Research Foundation.

References

[1] Padhi A K, Nanjundaswamy K S and Goodenough J B 1996 *Electrochem. Soc.* **96** 73
[2] Amatucci G G and Pereira N, 2007 *J. Flourine Chem.* **128** 243
[3] Ellis B L, Makahnouk W R M, Weetaluktuk W N R, Ryan D H and Nazar L F 2010 *J. Chem. Mater.* 22 1059
[4] Barker J, Saidi M Y and Swoyer J 2003 *J. Electrochem. Solid-State Lett.* **6** A1
[5] Zhou H, Wang X, Tang A, Liu Z, Gamboab S and Sebastian P J 2006 *J. Power Sources* **160** 698
[6] Lee K T, Ramesh T N, Nan F, Botton G and Nazar L F 2011 *Chem. Mater.* **23** 3593
[7] Shakoor R A, Park Y U, Kim J, Kim S W, Seo D H, Gwon H and Kang K 2010 *J. Korean Battery Soc.* **3** 00
[8] Mizushima K, Jones P C, Wiseman P J and Goodenough J B 1980 *Mater. Res. Bull.* **15** 799
[9] Amine K, Yashuda H and Yamachi M 2000 *Electrochem. Solid-State Lett.* **31** 179
[10] Pivko M, Bele M, Tchernychova E, Logar N Z, Dominko R and Gaberscek M 2012 *Chem. Mater.* **24** 1041
[11] Sauvage S, Quarez E, Trascon J M and Baudrin E 2006 *J. Electrochem. Soc.* **8** 1215
[12] Moreau P, Guyomard D, Gaubicher J and Boucher F 2010 *Chem. Mater.* **22** 4126
[13] Sun A and Manivannam A 2011 *ASC Transactions* **35** 3
[14] Moreau P, Guyomard D, Gaubicher F and Boucher F 2010 *Chem. Mater.* **22** 4126
[15] Kresse G and Furthmüller J 1996 *Phys. Rev. B* **54** 11169
[16] Kresse G and Joubert D 1999 *Phys. Rev.* **59** 1758
[17] Methfessel M and Paxton A 1989 *Phys. Rev. B* **40**, p. 3616
[18] Li G, Azuma H and Tohda M 2002 *Electrochem. Solid-State Lett.* **5** A135
[19] Le S N, Eng W and Navrotsky A 2006 *Solid State Chem.* **179** 3731
[20] Bridson J N, Quinlan S E and Tremaine P R 1998 *J. Chem. Mater.* **10** 763
[21] Wu Y 2015 Lithium-ion batteries, fundamentals and Applications *Tayor and Francis Group* Boca Raton

[22] Kinyanjui M K 2010 Electronic and Structural Properties of Li(1-x)FePO4 (X=0, 0.5,1) Ph.D. Thesis ULM University

[23] Fast L, Wills J M, Johansson B and Eriksson O 1995 *Phys. Rev. B* **51** 17431

[24] Sinko G V and Smirnov N A 2002 *J. Phys. Condens. Matter* **14** 6989

[25] Grimsditch M, Polian A, Brazhkin V and Balitskii D 1998 *J. Appl. Phys.* **83** 3018

[26] Patil S K R, Khare S V, Tuttle B R, Bording J K and Kodambaka S 2006 *Phys. Rev. B* **73** 104118

[27] Ravindran P, Fast L, Korzhavyi P A, Johansson B, Wills J and Eriksson O 1998 *J. App. Phys.* **84** 4904

[28] Chung H Y, Weinberger M B, Yang J M, Tolbert S H and Kaner R B 2008 *Appl. Phys. Lett.* **92** 261904

[29] McHargue C, Darby Jr J B, Yacaman M J and Gasga J R 1997 Norwell, Massachusetts, USA: Kluwer Academic Publishers

[30] Shein I R and Ivanovskii A L 2008 *J. Phys. Condens. Mater* **20** 415218

[31] Pugh S F 1954 *Philos. Mag.* **45** 833

[32] Wang D, Wu X, Wang Z and Chen L 2005 *J. Power Sources* **140** 125